NASA
Technical
Paper
3262

December 1992

Weight Optimization of an Aerobrake Structural Concept for a Lunar Transfer Vehicle

Lance B. Bush,
Resit Unal,
Lawrence F. Rowell,
and John J. Rehder

NASA

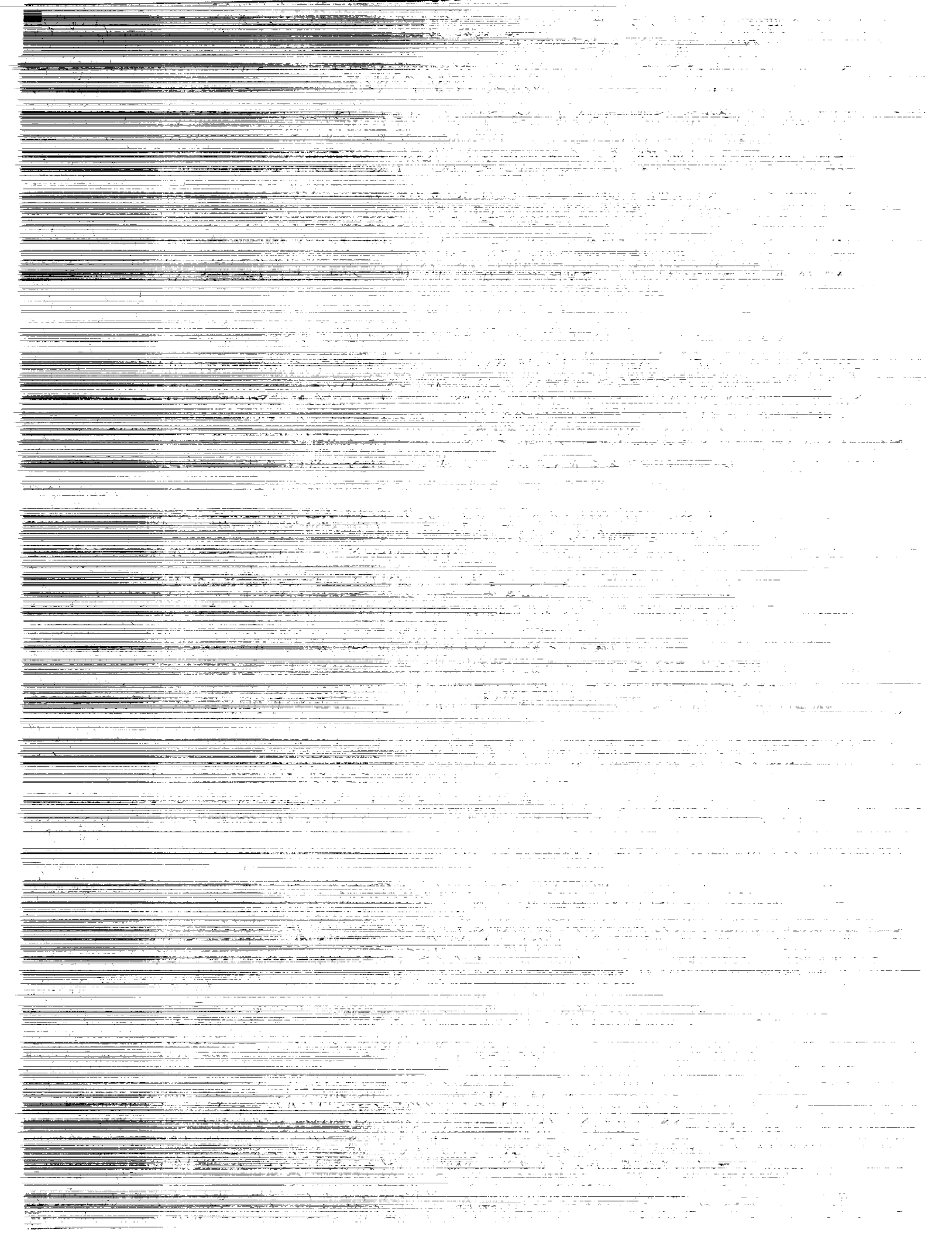

NASA Technical Paper 3262

1992

Weight Optimization of an Aerobrake Structural Concept for a Lunar Transfer Vehicle

Lance B. Bush
Langley Research Center
Hampton, Virginia

Resit Unal
Old Dominion University
Norfolk, Virginia

Lawrence F. Rowell
and John J. Rehder
Langley Research Center
Hampton, Virginia

National Aeronautics and Space Administration
Office of Management
Scientific and Technical Information Program

Nomenclature

A	area
APAS	Aerodynamic Preliminary Analysis System
Al	aluminum 2219
Al-Li	aluminum-lithium
C-C	carbon-carbon
D-D	diameter-depth (ratio)
E	ellipsoid
EAL	Engineering Analysis Language
EZDESIT	computer routine for finite element sizing
FEA	finite element analysis
L_{27}	ellipsoid Taguchi matrix (for 27 experiments)
LTV	lunar transfer vehicle
M	moment load
MMC	metal matrix composites
N	normal load
PATRAN	package for finite element modeling
POST	Program to Optimize Simulated Trajectories
S	spheroid
SEI	Space Exploration Initiative
SMART	Solid Modeling Aerospace Research Tool
S-C	sphere-cone
TPS	thermal protection system
t	thickness, in.
ΔV	change in velocity
W	weight, lb
x, y	coordinates
3-D	three-dimensional
ρ	density, lb/ft^2

Abstract

An aerobrake structural concept for a lunar transfer vehicle was weight optimized through the use of the Taguchi design method, finite element analyses, and element sizing routines. Six design parameters were chosen to represent the aerobrake structural configuration. The design parameters included honeycomb core thickness, diameter-depth ratio, shape, material, number of concentric ring frames, and number of radial frames. Each parameter was assigned three levels. The aerobrake structural configuration with the minimum weight was 44 percent less than the average weight of all the remaining satisfactory experimental configurations. In addition, the results of this study have served to bolster the advocacy of the Taguchi method for aerospace vehicle design. Both reduced analysis time and an optimized design demonstrated the applicability of the Taguchi method to aerospace vehicle design.

1. Introduction

A lunar colony is one mission among many being studied as part of the Space Exploration Initiative (SEI). (See ref. 1.) The economical transportation of materials and personnel from Earth to the Moon in support of a lunar colony constitutes a major technical challenge. A method of minimizing the overall transportation costs is through the use of efficient, space-based, reusable lunar transfer vehicles (LTV's). The first LTV's were those of the Apollo missions and were ground based. For mission scenarios currently under consideration, LTV's supporting the lunar colony would be space based, thus eliminating recurring, low Earth-to-orbit launch costs. A space-based, reusable LTV would reside at the Space Station *Freedom* or a space platform and transfer payloads between its docking residence and the Moon.

Lunar missions require large changes in velocity (ΔV's) in order to transfer from the lunar return orbit to the Earth parking orbit (ref. 2). These types of maneuvers are referred to as orbit capture. Two primary methods are used to achieve capture. The current capture method is through the use of propulsion (fig. 1) and has been used for all NASA planetary missions to date. To attain the necessary ΔV's for Earth orbit capture upon lunar return, a large amount of propellant is needed and must be carried for the entire trip (from Earth to the Moon and back).

An aerobraked LTV (fig. 2) offers an alternative method by attaining the necessary ΔV through an aerodynamic approach in which the need for a propulsive capture burn at Earth perigee is eliminated. An aerobrake grazes the atmosphere at Earth (fig. 3) by utilizing drag to decrease velocity for capture. One class of aerobrakes are curved surfaces (large enough to protect the spacecraft from hot gases in the wake) that are shaped so as to provide the necessary lift, drag, and controllability. The concave side of the aerobrake is fitted with the spacecraft, and the convex side is the aerodynamic surface upon which aerodynamic forces act to slow the vehicle upon entry into the atmosphere.

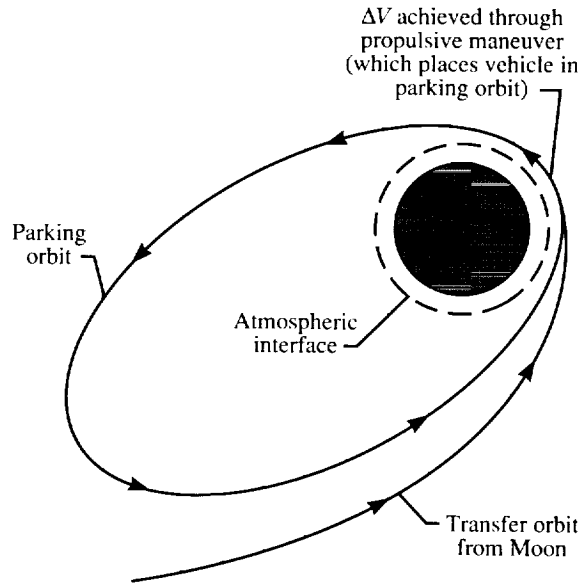

Figure 1. Propulsive capture.

A significant portion of all LTV's consist of propellant tanks (fig. 2). (See ref. 3.) By utilizing an aerobraking device instead of a propulsive burn for capture, a significant amount of propellants can be saved. Figure 2 shows the difference in size and tankage between an LTV with and without an aerobrake.

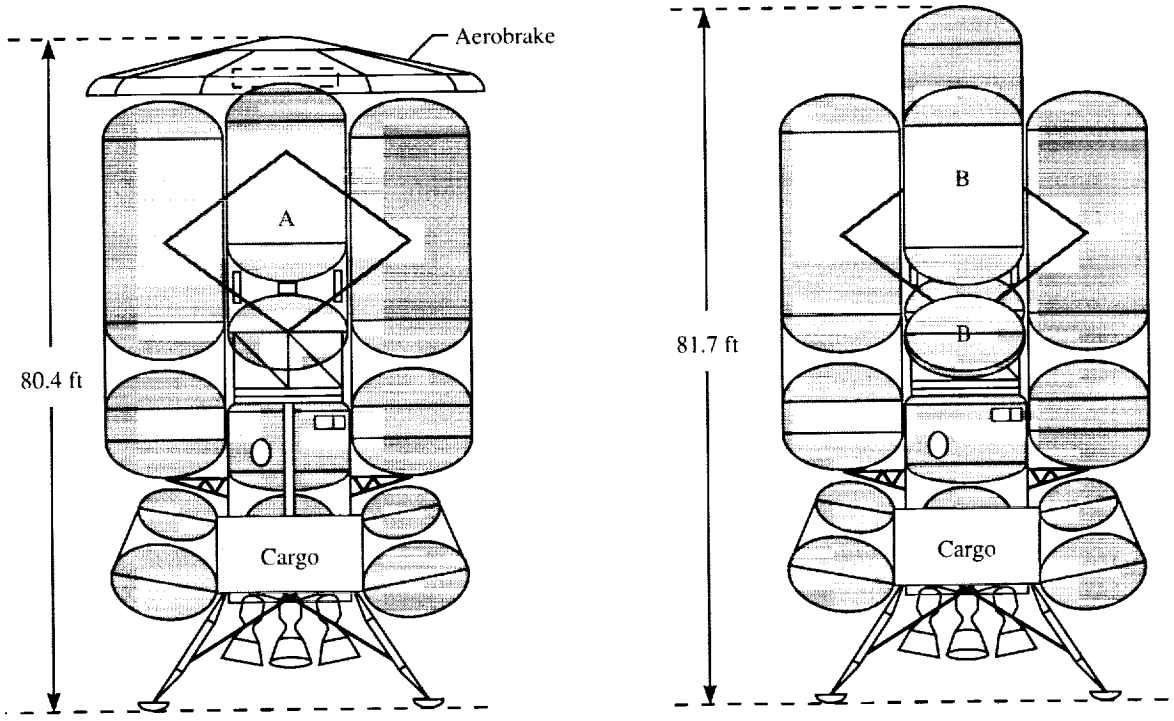

(a) LTV with aerobrake. A denotes one tank.

(b) All-propulsive LTV. B denotes two tanks (front and back).

Figure 2. Lunar transfer vehicle configurations (ref. 4).

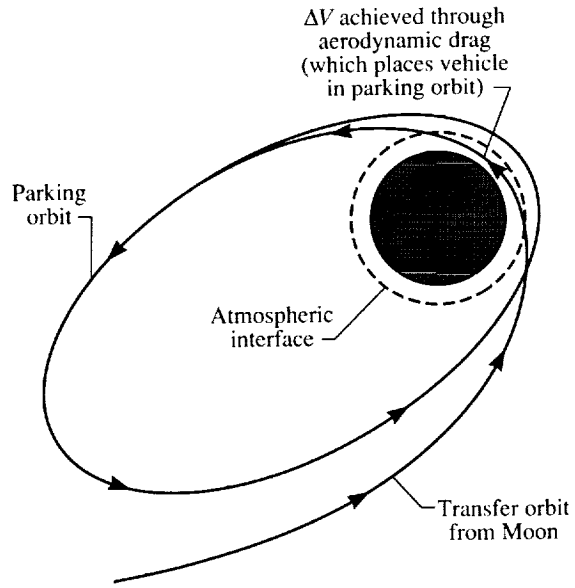

Figure 3. Aerodynamic capture.

In figure 2(b) the aerobrake is replaced with a significant amount of propellants and the size of the LTV has increased. Studies show that the number of shuttle launches to deliver the LTV to orbit can be reduced from three to two when substituting an aerobrake configuration for an all-propulsive configuration (ref. 4). Thus, if an aerobrake can be used to aerodynamically achieve the necessary ΔV's, a significant mass savings may be realized. An aerobrake can be considered advantageous from a performance standpoint only if the aerobrake mass is less than the mass savings of the propellant and propulsion system. Thus, the structural concept, material selection, and other design features must be optimized to produce a minimum-weight aerobrake that meets performance requirements.

Typically in the past, a basic structural analysis configuration was defined by the experience and engineering judgment of the designer. Within the time constraints of the study, simple design variable (parameter) trades would be performed. In these trades, analyses are performed when the value of one design variable (a parameter level) is altered while all other design variables are left constant. This approach has been necessary when considering the time constraints and the lack of a strong physical definition of a concept at the time of conceptual-preliminary level design. In addition, this approach does not identify the possible interaction of the parameters. Varying several design parameters simultaneously may have interactive effects on the design objective, which can

affect the optimum solution. When the effect of one parameter depends on the level of another, an interaction is said to exist. The study of parameter interactions is important in order to determine the optimum case. A full factorial approach, where all combinations of all parameters are analyzed, could find the near-optimum configuration, but it would be too time consuming.

The Taguchi methodology offers an attractive alternative by providing a systematic, economical method for reducing the number of analysis configurations. Using orthogonal arrays, the Taguchi method explores the entire design space through a small number of experiments in order to determine all the parameter effects and several of the interactions. These data are then used to predict the optimum combination of the design parameters that will minimize the objective function and satisfy all the constraints. In addition to locating a near-minimum objective function, the Taguchi method provides information on parameter trends, thereby enabling a robust design. Furthermore, both discrete and continuous variables can be studied. The Taguchi method employs the use of orthogonal arrays based on the *design of experiments theory*. The design of experiments theory was developed in Great Britain in the 1940's for the improvement of crop production (ref. 5). Taguchi institutionalized the approach by creating a handbook of standard orthogonal arrays (ref. 6). The Taguchi method was then utilized in Japan to revolutionize the consumer product market, specifically, electronics (ref. 7). This approach has been used in other industries, but it has just recently been utilized for aerospace design (ref. 8).

Fully stressed structural analysis techniques and a Taguchi design methodology are utilized in this study to identify a lunar minimum-weight aerobrake structural design and the associated design parameter sensitivities. This study focuses on structural design, although the total aerobrake design considers iterative input from other disciplines such as aerodynamics, performance, weight, packaging, and heating. The twofold objective of this study is to obtain a minimum-weight aerobrake structural configuration and demonstrate the applicability of the Taguchi method for aerospace vehicle structural design.

2. Inputs and Assumptions

Prior to this structural design and analysis study, aerodynamic analyses and a configuration layout study were performed in order to establish performance requirements and determine viable shapes for an aerobrake similar to that in figure 2(a). Hundreds of variations of four basic shapes were tested including spheroids, ellipsoids, hyperboloids, and sphere-cone configurations; they were described by several geometric parameters including effective nose radius, cone angle, diameter-depth ratio, etc. Configuration layout studies addressing fit within the wake flow and center-of-gravity placement resulted in a baseline aerobrake diameter of 50 ft and a 40 000-lb cylindrical payload with a diameter of 25 ft. The aerodynamic analyses of the selected shapes were performed at flight conditions having a Mach number of 20 and an altitude of 200 000 ft in order to match the flight-entry corridor for aerobraking trajectories that were constrained to an inertial loading of $5g$ acceleration (where $1g \approx 32.174$ ft/sec^2).

The inertial and aerodynamic loads incurred during the mission are utilized as the design loading conditions. Ground operations, maintenance, handling, and transportation have yet to be defined for the aerobrake vehicle, and the loads incurred during manufacturing, transportation, and maintenance are reserved for further studies.

In order to perform a timely study, only those parameters envisioned as having the greatest effect on the aerobrake weight were selected for analysis. The levels for these parameters were selected based on preliminary study results or engineering judgment. A description of the parameters and their levels follows.

A skin/stringer structural configuration is chosen to represent the aerobrake (fig. 4). Honeycomb sandwich panels with a frame network, isogrid panels,

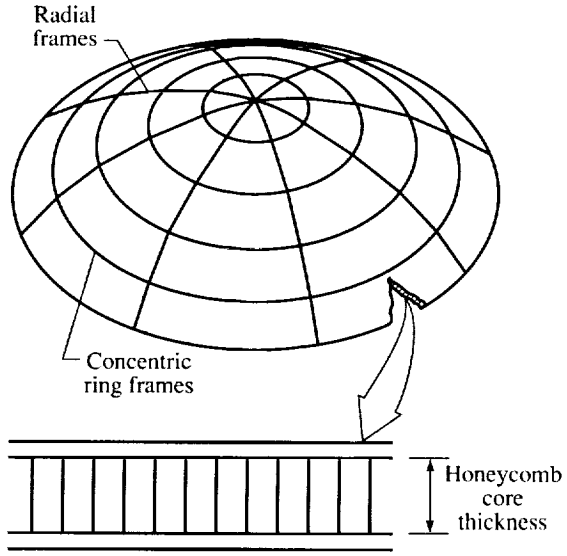

Figure 4. Concentric ring frames (rings), radial frames (frames), and honeycomb core thickness.

and a membrane skin with a complex truss structure arrangement are all alternatives. The honeycomb sandwich with a frame network was selected for this conceptual-preliminary level assessment based on its past performance (ref. 9). The levels for honeycomb depth were based on the preliminary tests described in section 4 of this study.

Stiffeners for the aerobrake include radial frames and concentric ring frames. Stiffener directions were selected to match the major load paths of the vehicle (hoop and radial). These frames were modeled as I-beams with a web height of 6 in., a cap width of 1 in., and a cap and web thickness of 1/10 in.

The launch configuration of the aerobrake vehicle is dependent upon the packaging constraints of the Earth-to-orbit launch vehicle. Little definition exists of the on-orbit assembly method and mechanisms for aerobrakes. Thus, the joint mass for this concept is not addressed because of the lack of definition and data in this area.

The three materials selected for the aerobrake structure are aluminum 2219 (Al), aluminum-lithium (Al-Li), and carbon-carbon (C-C). These three materials represent three different levels of technology (i.e., conventional, near-term, and advanced, respectively).

Aerobrakes must be capable of surviving the high-temperature environments occurring during atmospheric reentry. Thermal analysis of a 45-ft-diameter sphere-cone aerobrake with a 10-ft-radius nose cone and a 20° cone sweep angle indicates a peak surface temperature of 3200°F (fig. 5). The temperature performance (fig. 6) of aluminum and aluminum-lithium structures dictates a need for a thermal protection system (TPS). (See ref. 10.)

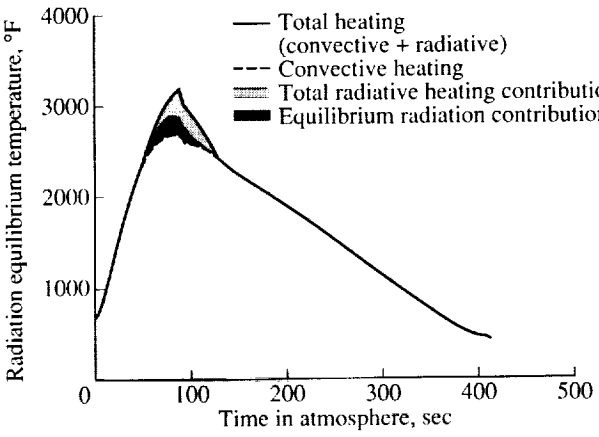

Figure 5. Heating of sphere-cone aerobrake for lunar return. Aerobrake had 45-ft diameter, 10-ft-radius nose, and 20° cone sweep angle.

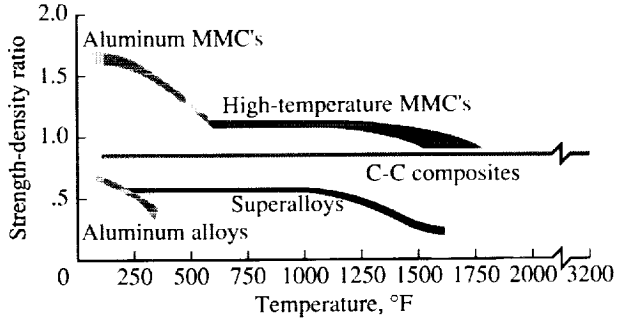

Figure 6. Temperature performance of materials.

The additional weight of the TPS will be added to the final structural weight of the aluminum-based configurations with the result that a reasonable comparison can be made with the weight of the carbon-carbon configuration which needs no additional TPS. The selected TPS must satisfy on-orbit installation, repair, refurbishment, and inspection requirements; and thus the best insulating requirements or lowest mass options may not be met. Yet, because no specifications of these on-orbit requirements exist at present, the TPS will be chosen for analytical purposes on the basis of its thermal and mass characteristics.

A survey of various TPS systems indicates that an aluminum-enhanced thermal barrier TPS with an average area mass density of 1.75 lb/ft^2 and a uniform thickness of 3/8 in. may be assumed to fulfill the temperature and thermal gradient considerations shown in figure 5. The mass density includes the weight of an aluminum carrier plate, a Du Pont Nomex pad, and a room-temperature vulcanized compound. The tile exterior is coated with alumina (aluminum oxide), a 1/10-in. thickness of alumina felt, and a protective coating of carbon silicon carbide with carbon fibers.

As a result of these assumptions, the six parameters chosen to represent the design variables of the aerobrake configuration include shape, diameter-depth ratio, honeycomb core thickness, number of radial frames, number of concentric ring frames, and material (table I).

3. Design and Analysis Methodology

3.1. Study Matrix

If the six design variables are each defined at three levels, a full study matrix for all possible combinations would require 3^6, or 729, analysis cases. A systematic approach to selecting an appropriate subset of these is needed.

Table I. Design Parameters and Levels

Parameter level	Honeycomb core thickness, in.	Number of radial frames	Number of ring frames	Material	Shape	Diameter-depth (D-D) ratio
1	2.75	5	4	Al	E	4
2	3.00	10	7	Al-Li	S	6
3	3.25	20	10	C-C	S-C	8

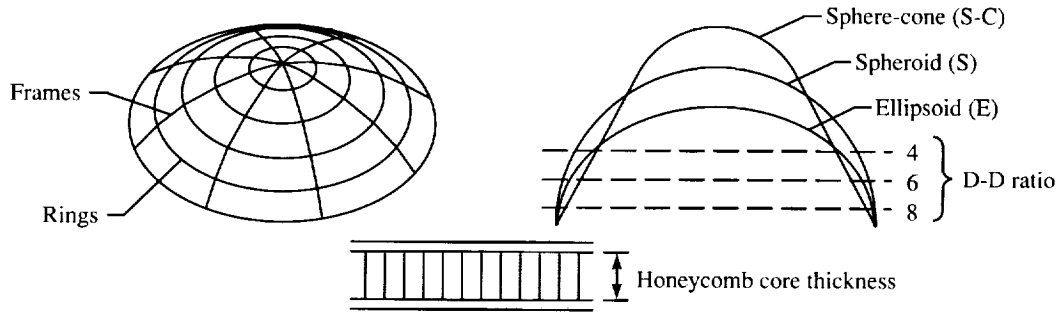

The Taguchi method uses orthogonal arrays from the design of experiments theory to study the parameter space with a significantly small number of experiments. Taguchi has tabulated 18 standard orthogonal arrays. In many cases, one of these arrays can be used directly or can be modified to fit a specific project. To select the appropriate orthogonal array to fit a specific case study, we need to count the total degrees of freedom to find the minimum number of experiments that must be performed to reach a near-optimum parameter set.

One degree of freedom is associated with the overall mean regardless of the number of design parameters. A three-level parameter counts for two degrees of freedom. The degrees of freedom associated with interaction between two parameters is given by the product of the degrees of freedom for each of the two parameters. Therefore, we have 12 degrees of freedom because of the 6 parameters and 12 degrees of freedom because of parameter interactions, resulting in a total of 24. In order for an array to be a viable choice, the number of rows must at least be equal to the degrees of freedom required for the case study.

Hence, an L_{27} array (having 27 rows) was selected (table II). This array has 26 degrees of freedom, and it can handle 7 parameters at 3 levels and 3 interactions between 2 parameters. One column is necessary to represent each parameter, and two columns for each parameter interaction. Since only 6 parameters and 3 interactions occur, 12 of the 13 available columns will be used. Orthogonality is not lost by keeping one or more columns of an array empty. For this study, the utilization of an L_{27} array reduced the number of experimental configurations from 729 (required by a full factorial study) to 27.

The Taguchi design methodology for this study employs the following seven basic steps (refs. 11 and 12):

1. Identify the design parameters and their alternative levels.
2. Define possible interactions between these parameters.
3. Select an appropriate Taguchi orthogonal array.
4. Determine the parameter arrangement.
5. Conduct the matrix experiment (by using the appropriate finite element analysis).
6. Create response tables and graphs, and analyze the data.
7. Determine the optimum levels for the design parameters, and then verify.

In step 1, selection of the design parameters and their corresponding levels determines the design space. This is an important step. The Taguchi method will determine the combination of the parameter levels that gives the near-optimum performance (i.e., low weight) and the sensitivity of the results to the parameters within the given design space.

Table II. L_{27} Taguchi Matrix[a]

Experiment number	Parameter levels for each experiment at columns—												Results		
	①	②	③	④	⑤	⑥	⑦	⑧	⑨	⑩	⑪	⑬			
	Shape	Honeycomb	① × ②	① × ②	Material	⑤ × ①	⑤ × ①	② × ⑤	Frames	Rings	② × ⑤	D-D ratio	Aerobrake weight, lb	Aerobrake weight + TPS, lb	Global buckling eigenvalue
1	1	1	1	1	1	1	1	1	1	1	1	1			
2	1	1	1	1	2	2	2	2	2	2	2	2			
3	1	1	1	1	3	3	3	3	3	3	3	3			
4	1	2	2	2	1	1	1	2	2	2	3	3			
5	1	2	2	2	2	2	2	3	3	3	1	1			
6	1	2	2	2	3	3	3	1	1	1	2	2			
7	1	3	3	3	1	1	1	3	3	3	2	2			
8	1	3	3	3	2	2	2	1	1	1	3	3			
9	1	3	3	3	3	3	3	2	2	2	1	1			
10	2	1	2	3	1	2	3	1	2	3	1	3			
11	2	1	2	3	2	3	1	2	3	1	2	1			
12	2	1	2	3	3	1	2	3	1	2	3	2			
13	2	2	3	1	1	2	3	2	3	1	3	2			
14	2	2	3	1	2	3	1	3	1	2	1	3			
15	2	2	3	1	3	1	2	1	2	3	2	1			
16	2	3	1	2	1	2	3	3	1	2	2	1			
17	2	3	1	2	2	3	1	1	2	3	3	2			
18	2	3	1	2	3	1	2	2	3	1	1	3			
19	3	1	3	2	1	3	2	1	3	2	1	2			
20	3	1	3	2	2	1	3	2	1	3	2	3			
21	3	1	3	2	3	2	1	3	2	1	3	1			
22	3	2	1	3	1	3	2	2	1	3	3	1			
23	3	2	1	3	2	1	3	3	2	1	1	2			
24	3	2	1	3	3	2	1	1	3	2	2	3			
25	3	3	2	1	1	3	2	3	2	1	2	3			
26	3	3	2	1	2	1	3	1	3	2	3	1			
27	3	3	2	1	3	2	1	2	1	3	1	2			

[a] ① × ② = Interaction of honeycomb core thickness and shape.

⑤ × ① = Interaction of shape and material.

② × ⑤ = Interaction of honeycomb core thickness and material.

In step 2, possible interactions between the design variables are selected for investigation based on experience. The Taguchi method can determine the existence of these interactions. If interactions are not correctly identified at this stage, the study will indicate this deficiency with inconsistent results at the verification stage. If this occurs, the design process must be restarted with new interactions selected.

In step 3, an appropriate Taguchi matrix is selected. Standard Taguchi matrices exist in reference handbooks (ref. 7). The selected matrix must accommodate the parameters, their levels, and the interactions. The matrix must contain at least one column for each parameter and each interaction. The number of levels will determine the number of rows in a matrix.

In step 4, the parameter arrangement in the matrix is determined. The arrangement is dependent upon the chosen parameter interactions. For more details on parameter arrangement, see reference 13.

In step 5, the matrix experiments are conducted. The experimental method is dependent on the nature of each problem. For this study, the experimental procedure is conducted by performing a finite element analysis of each experimental configuration. A finite element structural analysis yields estimates of stress and resultant loads on the structures under external loading conditions. This procedure is described in section 3.2.

In step 6, the result for each experiment is listed and an average value is calculated for each experiment having a specified parameter level. A comparison of the average results for one level with those of the other levels within a parameter indicates the sensitivity due to that specific parameter. The difference between the greatest and least average values for each parameter gives an indication of the relative degree of sensitivity when compared with the difference for other parameters. For parameters whose interactions are not studied, the optimum level is identified by the lowest averaged result. Analysis of interacting parameter results is more complex, and thus it is reserved for a later explanation.

In step 7, the optimum levels for the parameters are chosen and verification tests are made. Further experimentation can be attempted if the sensitivity graphs indicate that any further optimization is possible outside the original design space.

3.2. Methodology of Analysis

A finite element modeling and analysis technique is utilized to determine the integrity of each aerobrake structural arrangement. Of primary concern is the ability of each candidate structure to resist local mechanical failure modes and global buckling (eigensolution) when subjected to aerodynamic and inertial loading present during the mission. Thus, each configuration analysis includes geometry modeling, finite element modeling, aerodynamic pressure distribution, inertial loads application, finite element analysis, structural element sizing, structural element weight summation, and postprocessing results evaluation (fig. 7).

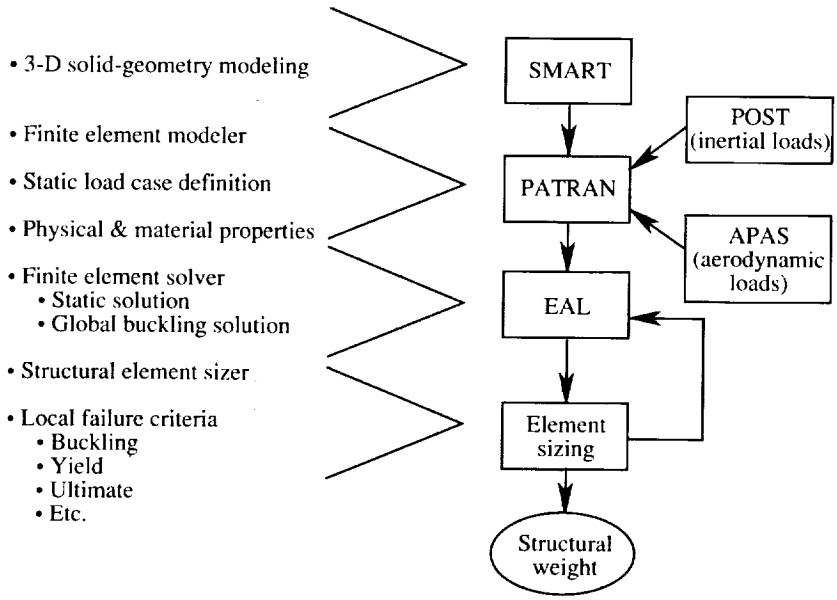

Figure 7. Structural analysis procedure.

The geometry concepts are modeled through the use of the Solid Modeling Aerospace Research Tool (SMART) system. (See ref. 14.) The models are stored as bicubic patch data used in both the finite element and aerodynamic analyses.

The structural finite element model is derived by discretizing the SMART-generated external surface geometry. Internal structural arrangements, or frames, are incorporated within the computer program PATRAN for finite element modeling. (See ref. 15.) These structures are incorporated into the vehicle to withstand the external loading and provide safe loading paths, thus making the vehicle capable of completing the mission without structural failure. The desired section and material properties of the structure are also included in the finite element model of the vehicle at this point.

Typically, the external geometry of a candidate configuration is determined by the results of aerodynamic studies aimed at achieving necessary or optimum aerodynamic characteristics. The aerodynamic analysis is performed utilizing a modified Newtonian technique included in the Aerodynamic Preliminary Analysis System (APAS) code. (See refs. 16 and 17.) Aerodynamic surface pressures are calculated and mapped from the aerodynamic model onto the structural finite element model.

The aerodynamic loads combine with the inertial loads calculated through a performance analysis to simulate the critical mission loading conditions. The inertial acceleration vectors are calculated by utilizing Program to Optimize Simulated Trajectories (POST). (See ref. 18.) With the addition of the external loading, the finite element structural model is complete and is ready for analysis.

Finite element analysis (FEA) is performed on the finite element model in order to determine the resulting loads due to the mission loading conditions. FEA is performed utilizing the Engineering Analysis Language (EAL). (See ref. 19.) The FEA produces resultant structural loads for each finite element. These resultant loads are indicative of the load paths and integrity of the vehicle structure and may indicate areas of the vehicle that are loaded beyond the limits of the construction material.

These loads are used as input to a structural sizing routine in order to determine the changes necessary in section properties (i.e., plate thickness and bar diameter) to meet failure criteria. Each structural element (bars, planar beams, and plate elements) is sized within the EZDESIT computer program to withstand the mission loading conditions (fig. 8). (See ref. 20.)

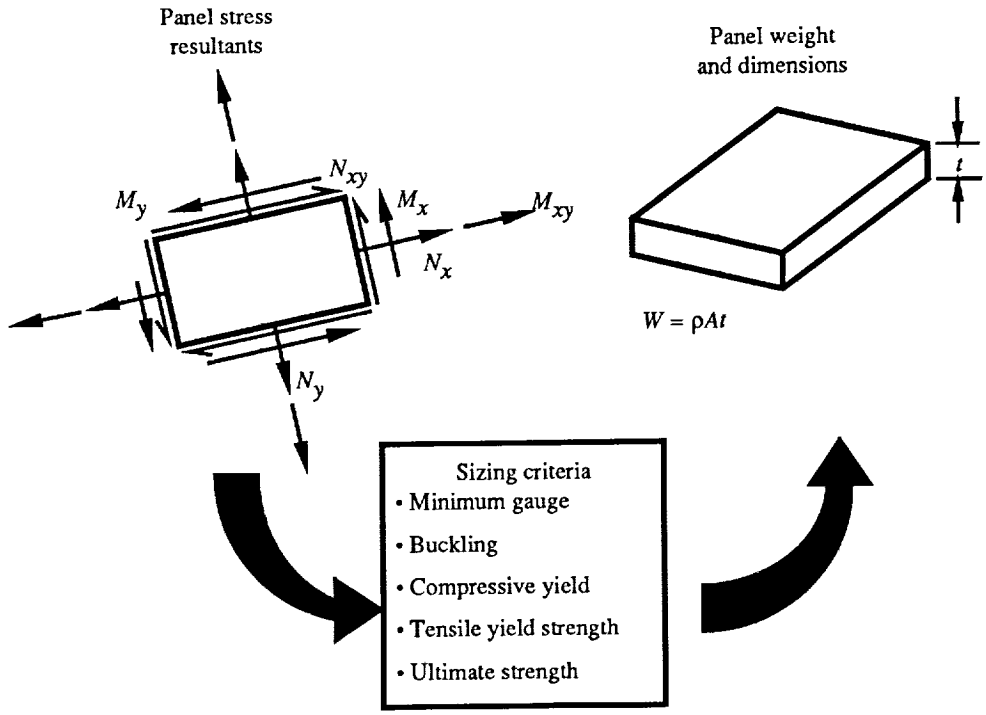

Figure 8. EZDESIT finite-element-sizing methodology for flat plate.

The weights of all the structural finite elements are added to obtain the structural weight of the aerobrake. The geometric sizing of the structural elements alters the stiffness properties of the aerobrake finite element model. Thus, the finite element analysis and structural element sizing are iterated until an aerobrake weight convergence is achieved. A convergence occurs when the difference between the structural weight of two consecutive iterations is negligible. A converged solution typically takes three iterations.

The results of the sizing can be reviewed in two manners. An interactive session of the EZDESIT program permits the designer to review the data in tabular form. The weight of the aerobrake structure is calculated and displayed by component, load case, failure mode, and element type. In the second method, the EZDESIT results are read into PATRAN, a finite element preprocessor and postprocessor, and the structural element results are displayed graphically on the model. These include resulting loads, dominant load case, failure modes, and unit weights. Highly loaded areas may indicate a need for an alternative structural design. Resultant loads are reviewed by the structural designer, and if necessary, changes to the structural arrangement are made by altering the finite element model and reanalyzing the structure.

Each finite element model is checked for global buckling. The eigensolver routine in EAL is utilized to determine the percent of static loads necessary to obtain a globally buckled model. When the eigenvalue is less than 1, the loads are too great and global buckling occurs. Thus, an optimum configuration would attain a global buckling eigenvalue of 1.

4. Preliminary Results

A few aerobrake concepts were analyzed prior to establishing the design matrix to determine a reasonable range of parameter values. These preliminary results show that the relationship between honeycomb thickness variation and global buckling is sensitive (fig. 9). This analysis was conducted for a 37.5-ft-diameter aerobrake with a diameter-depth ratio of 1.5 and an eccentricity of 0.5. The aerobrake model assumed a honeycomb construction of aluminum 2219 with 4 concentric ring frames, 10 radial frames, and a factor of safety of 1.5. According to figure 9, a honeycomb thickness of at least 2.64 in. is necessary to maintain structural integrity. Based on these results, a minimum honeycomb thickness of 2.75 in. was selected. Results indicated that global buckling was the primary failure criterion. Localized phenomena such as yield and ultimate stresses were less important. The number of concentric ring frames and radial frames along with the honeycomb thickness has an effect on global buckling. Thus, emphasis was placed on these variables in an attempt to alleviate the global buckling phenomenon.

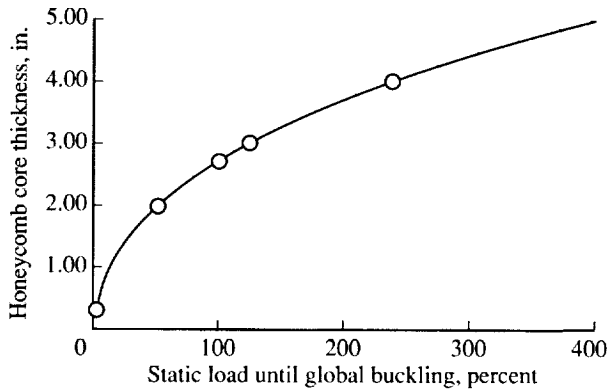

Figure 9. Honeycomb core thickness of elliptical aerobrake as function of global buckling. Aerobrake had diameter of 37.5 ft, eccentricity of 0.5, depth of 25 ft, and was made of aluminum 2219.

5. Design Matrix

A design space for Taguchi optimization is defined by selecting design parameters and setting their levels. The design parameters and their levels are chosen based upon experience and knowledge. Inappropriate choices of parameter levels will incur the need for further analyses. For this study, the selection process was impacted by aerodynamic, packaging, structural, and material concerns. A description of the decision process follows.

As mentioned previously, hundreds of aerobrake shapes were analyzed to determine their aerodynamic performance. The number of candidate configurations was reduced on the basis of their packaging efficiencies constrained by wake turning angle and aerodynamic performance requirements. Still, many candidate shapes remained viable. No further aerodynamic or performance criteria were applied to reduce the number of candidates. The selection from these viable candidates then was to be based on structural and weight considerations. Thus, the structural analysis was used as a design tool for the aerobrake selection. So many configurations remained that an orderly and efficient analysis method was necessary.

Based on the Taguchi method, the number of analysis configurations was reduced. Having the geometric characteristics of the aerobrakes chosen for analysis to represent the range of viable configurations was desirable. The entire design space was

represented with nine configurations that consisted of permutations of three shapes and three diameter-depth ratios varying from 4 to 8 (figs. 10–12). The three shapes were ellipsoid, spheroid, and sphere-cone. The ellipsoidal aerobrakes have an eccentricity of 0.5 (fig. 10). The sphere-cone aerobrakes are a composition of a spheroidal nose faired into a cone frustum. The sphere-cone aerobrakes have an effective nose radius of 24 ft and a cone angle varying from 60° to 75° (fig. 11). The spheroidal aerobrakes have an effective nose radius varying from 32 to 64 ft (fig. 12).

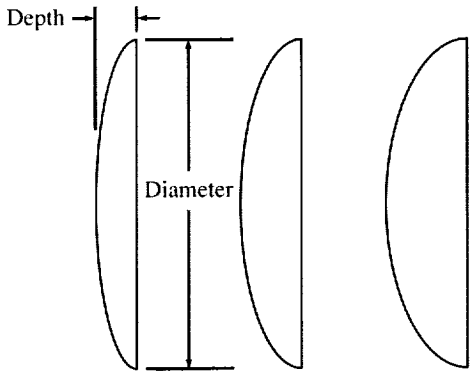

D-D ratio.....	8	6	4
Effective nose radius, ft...	110	83	63

Figure 10. Ellipsoidal aerobrakes. Eccentricity = 0.5.

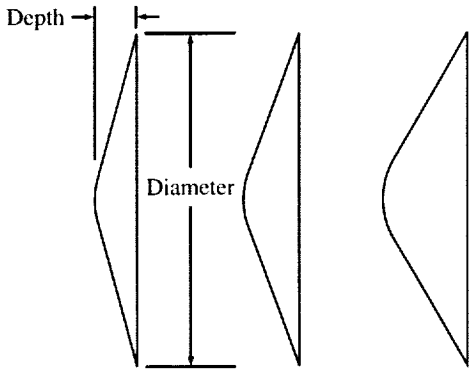

D-D ratio.....	8	6	4
Nose radius, ft.....	24	24	24
Cone angle, deg.....	75	70	60

Figure 11. Sphere-cone aerobrakes.

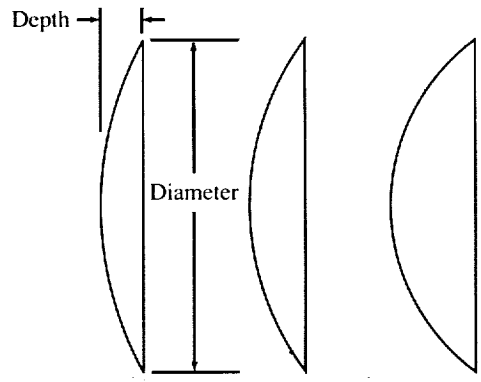

D-D ratio.....	8	6	4
Nose radius, ft...	64	48	32

Figure 12. Spherical aerobrakes.

The material selection is based on the projected technology availability. Three materials were chosen, each to represent a different level of technology. Aluminum was chosen to represent a state-of-the-art material. Aluminum-lithium was chosen to represent a near-term technology material. Carbon-carbon was selected to represent an advanced technology material.

Shape, diameter-depth ratio, and material are aerodynamic, packaging, and technology parameters, respectively, that impact the structural definition and weight of the aerobrake. The structural parameters include honeycomb thickness, number of radial frames, and number of ring frames. The design composed of these parameters will dictate the structural integrity of the models.

Based on the preliminary results discussed in section 4, the honeycomb-thickness levels chosen were 2.75, 3.00, and 3.25 in.

The minimum number of radial frames was based on the number of payload-to-aerobrake attachment points, which was assumed to be five. The five attachment points are placed a radial distance of 25 ft from the center and circumferentially at every 72°. This arrangement matches the assumed cylindrical payload dimensions and design. To ensure consistency across the finite element models, all are constructed with the same number of radial and circular surface elements. Therefore, to increase the number of evenly distributed radial frames while maintaining the five aerobrake-payload interfaces, the frames must be increased twofold. The number of radial frames at level 2 is 10 and at level 3 is 20.

The number of concentric ring frames for testing is 4, 7, and 10. This range of values gives a sparse,

medium, and dense distribution, respectively, of concentric ring frames.

The three pairs of interactions chosen for study involved all combinations of material, shape, and honeycomb thickness.

Given the six design parameters, their three interactions, and three levels, an L_{27} Taguchi matrix was selected (table II). Parameters require 1 column and interactions require 2, with the result that only 12 of the 13 columns associated with an L_{27} were needed. The arrangement of the parameters and their levels is represented generically by the letters and numbers. Table III shows the matrix combinations forming the actual experiments. (Interactions are not shown.) Each row represents an experiment, i.e., one combination of parameter levels.

6. Results

The analysis results of the 27 experiments are shown in table IV. These results vary from a maximum of 10 144 lb to a minimum of 4351 lb. The experiments include aerobrakes with aluminum, aluminum-lithium, and carbon-carbon structures. To compare the weights of these various material concepts fairly, a thermal protection system (TPS) weight is added to the aluminum and aluminum-lithium concepts but not to the carbon-carbon concept because this material can tolerate extremely high temperatures and operates as a hot structure. The TPS weight is calculated as the product of the surface area and the prior-established TPS unit weight.

Table III. Experiment Matrix

	Parameter level values for each experiment at columns—						Results		
	①	②	⑤	⑨	⑩	⑬			
Experiment number	Shape	Honeycomb core thickness, in.	Material	Number of radial frames	Number of ring frames	D-D ratio	Aerobrake weight, lb	Aerobrake weight + TPS, lb	Global buckling eigenvalue
1	E	2.75	Al	5	4	4			
2	E	2.75	Al-Li	10	7	6			
3	E	2.75	C-C	20	10	8			
4	E	3.00	Al	10	7	8			
5	E	3.00	Al-Li	20	10	4			
6	E	3.00	C-C	5	4	6			
7	E	3.25	Al	20	10	6			
8	E	3.25	Al-Li	5	4	8			
9	E	3.25	C-C	10	7	4			
10	S	2.75	Al	10	10	8			
11	S	2.75	Al-Li	20	4	4			
12	S	2.75	C-C	5	7	6			
13	S	3.00	Al	20	4	6			
14	S	3.00	Al-Li	5	7	8			
15	S	3.00	C-C	10	10	4			
16	S	3.25	Al	5	7	4			
17	S	3.25	Al-Li	10	10	6			
18	S	3.25	C-C	20	4	8			
19	S-C	2.75	Al	20	7	6			
20	S-C	2.75	Al-Li	5	10	8			
21	S-C	2.75	C-C	10	4	4			
22	S-C	3.00	Al	5	10	4			
23	S-C	3.00	Al-Li	10	4	6			
24	S-C	3.00	C-C	20	7	8			
25	S-C	3.25	Al	10	4	8			
26	S-C	3.25	Al-Li	20	7	4			
27	S-C	3.25	C-C	5	10	6			

Table IV. Experiment Matrix With Results

Experiment number	Parameter level values for each experiment at columns— ① Shape	② Honeycomb core thickness, in.	⑤ Material	⑨ Number of radial frames	⑩ Number of ring frames	⑬ D-D ratio	Results: Aerobrake weight, lb	Aerobrake weight + TPS, lb	Global buckling eigenvalue
1	E	2.75	Al	5	4	4	5 110	9 838	1.05
2	E	2.75	Al-Li	10	7	6	4 690	8 639	.56
3	E	2.75	C-C	20	10	8	9 173	9 173	2.23
4	E	3.00	Al	10	7	8	5 123	8 866	.42
5	E	3.00	Al-Li	20	10	4	6 470	11 198	.82
6	E	3.00	C-C	5	4	6	7 842	7 842	5.41
7	E	3.25	Al	20	10	6	6 147	10 096	.75
8	E	3.25	Al-Li	5	4	8	4 463	11 656	.40
9	E	3.25	C-C	10	7	4	7 913	7 913	4.75
10	S	2.75	Al	10	10	8	5 330	9 241	.85
11	S	2.75	Al-Li	20	4	4	4 951	9 274	.54
12	S	2.75	C-C	5	7	6	5 145	5 145	2.48
13	S	3.00	Al	20	4	6	4 955	8 824	.90
14	S	3.00	Al-Li	5	7	8	4 756	8 667	.81
15	S	3.00	C-C	10	10	4	6 927	6 927	2.42
16	S	3.25	Al	5	7	4	5 453	9 775	.63
17	S	3.25	Al-Li	10	10	6	5 370	9 239	1.12
18	S	3.25	C-C	20	4	8	10 144	10 144	5.66
19	S-C	2.75	Al	20	7	6	5 190	8 921	.44
20	S-C	2.75	Al-Li	5	10	8	4 472	8 105	.25
21	S-C	2.75	C-C	10	4	4	7 224	7 224	2.58
22	S-C	3.00	Al	5	10	4	5 247	9 258	.55
23	S-C	3.00	Al-Li	10	4	6	4 351	8 082	.33
24	S-C	3.00	C-C	20	7	8	9 927	9 927	1.97
25	S-C	3.25	Al	10	4	8	4 856	8 489	.28
26	S-C	3.25	Al-Li	20	7	4	5 509	9 520	.58
27	S-C	3.25	C-C	5	10	6	8 662	8 662	2.57

Table V. Response Table

Parameter level	Weight, lb, for-- Honeycomb	Frames	Rings	Material	Shape	D-D ratio
1	8396	8772	9042	9257	9469	8992
2	8844	8291	8597	9376	8582	8384
3	9500	9676	9100	8107	8688	9363
Sensitivity	1104	(1385)	503	(1269)	887	979

The aerobrake weights then vary from a maximum of 11 656 lb to a minimum of 5145 lb. Global buckling eigenvalues vary from 5.66 to 0.25. These weights and global buckling values are used to derive the effects of each parameter on these critical values. An average weight is calculated for the 9 out of 27 experiments that exist at level 1 for a particular parameter. This step is repeated for levels 2 and 3 of that parameter. These averages are calculated for all the parameters and are listed in the response table (table V). The relative sensitivity of each parameter on the weight is determined by subtracting the smallest value from the largest value in each parameter column. The number of frames and the material selection show the highest sensitivity (shown by the circled values in table V) because the greatest effect on weight is realized by varying these parameters.

The optimum level for the three noninteracting parameters (frames, rings, and diameter-depth ratio) can be selected by choosing the level within that parameter column with the lowest value for weight. Frames, rings, and diameter-depth ratio give optimum results at level 2 (that is, 7 frames, 10 rings, and a diameter-depth ratio of 6). Too many rings or frames add unnecessary weight to the structure, whereas a small number of rings or frames reduces the overall stiffness of the structure and allows for global buckling. The weights of the rings and frames exhibit a "bucket" trend when plotted against design level (fig. 13).

The diameter-depth parameter also exhibits a bucket trend when plotted against weight. This trend may be explained by two phenomena. As the diameter-depth parameter is reduced, the amount of surface area is reduced, thereby reducing weight. Additionally, as the diameter-depth parameter is reduced, the effect of the loading is increased because of the flattened shape which tends to increase weight. The balance between these effects occurs when the diameter-depth ratio is 6.

Interacting parameters require an alternate method of determining the optimum level. For the three parameters for which interactions were examined (honeycomb thickness, material, and shape), the weight at level 1 of parameter 1 is plotted against all the levels of parameter 2 (fig. 14). A line is constructed connecting these data points. This is

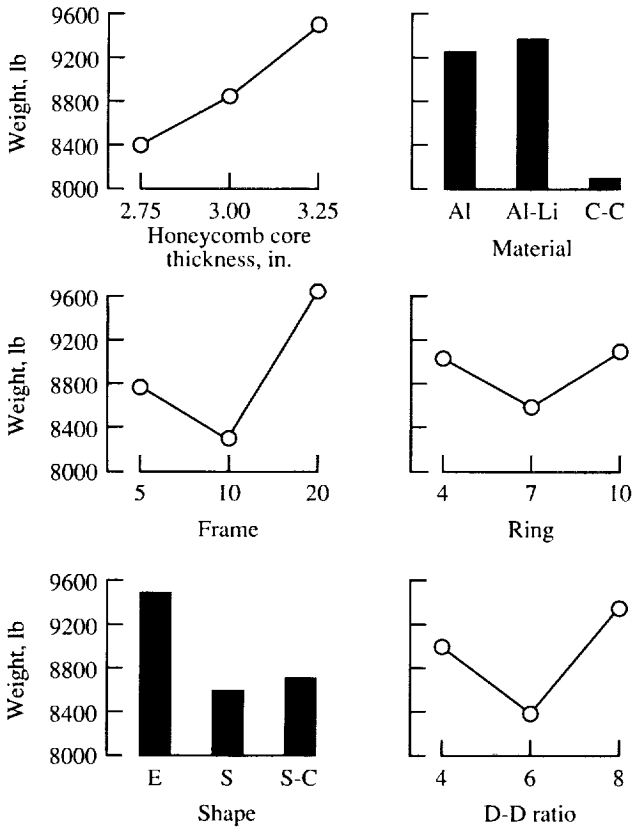

Figure 13. Response graphs.

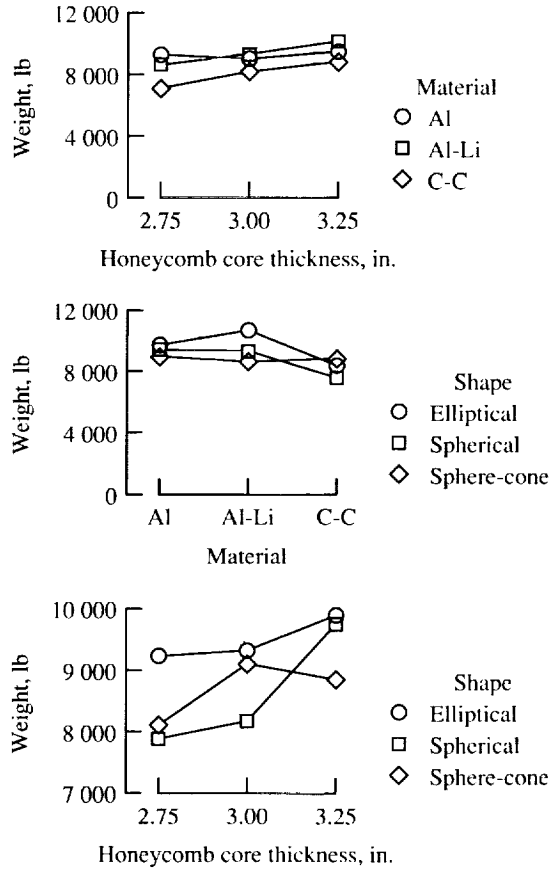

Figure 14. Interaction response graphs.

repeated on the same graph for levels 2 and 3 of parameter 1. If these lines are nonparallel, interactions occur; and if the lines cross, strong interactions occur between the parameters at these values. These plots verify that the strong interactions expected do indeed exist.

The parameter levels for the lowest weight combination for each graph are chosen as optimum levels. The interaction graph showing honeycomb thickness plotted against material displays an optimum combination of honeycomb thickness at level 1 (2.75 in.) and a material level of 3 (carbon-carbon). The interaction graph showing honeycomb thickness plotted against shape displays an optimum combination of honeycomb thickness at level 1 (2.75 in.) and a shape level of 2 (spheroid). The interaction graph of material plotted against shape displays an optimum combination of material at level 3 (carbon-carbon) and a shape level of 2 (spheroid).

The optimum parameter levels for a minimum weight configuration of the aerobrake structure are circled in table VI. This combination of parameter levels represents the optimum combination within the prescribed design space. A review of the sensitivity plots for weight (fig. 15) and global buckling (fig. 16) shows that additional weight benefits may be realized by further reducing the honeycomb thickness. The honeycomb core thickness cannot be reduced after the global buckling eigenvalue of 1.0 is reached (fig. 16). The results in figure 16 are for the Taguchi matrix experiments prior to selecting the optimum configuration. Therefore, the aerobrake was analyzed at four reduced honeycomb thicknesses while maintaining the optimum levels for all other parameters. (See table VII.) As the honeycomb core thickness is reduced, the aerobrake weight is reduced and global buckling is being approached. A final honeycomb core thickness of 2.00 in. still satisfied

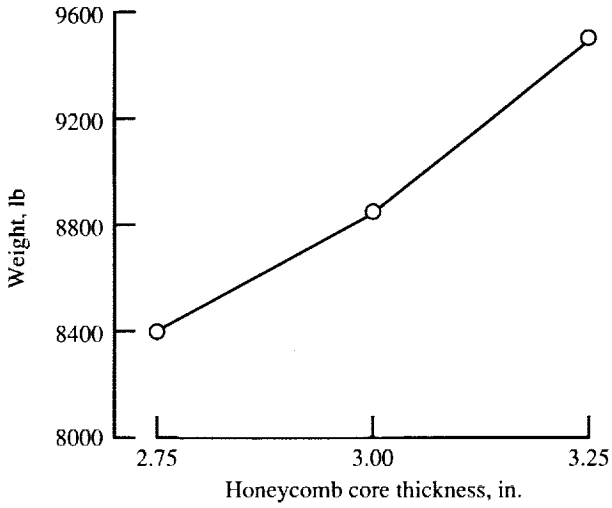

Figure 15. Weight sensitivity of honeycomb core thickness.

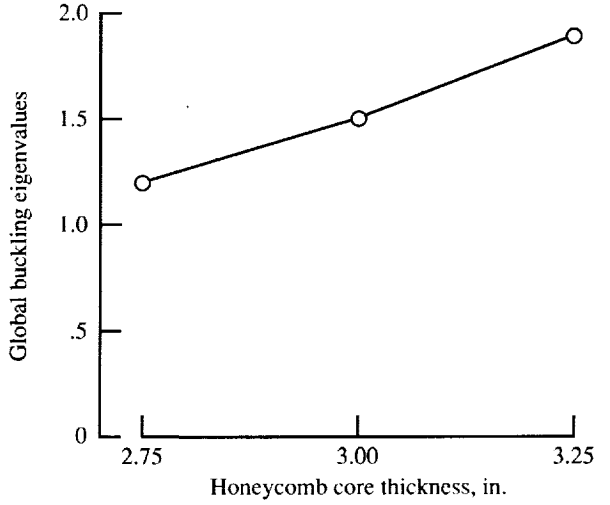

Figure 16. Global buckling sensitivity of honeycomb core thickness.

Table VI. Optimum Parameter Levels for Minimum Weight Configuration

Parameter level	Honeycomb core thickness, in.	Number of radial frames	Number of ring frames	Material	Shape	D-D ratio
1	(2.75)	5	4	Al	E	4
2	3.00	(10)	(7)	Al-Li	(S)	(6)
3	3.25	20	10	(C-C)	S-C	8

Table VII. Honeycomb Thickness Optimization

Honeycomb core thickness, in.	Weight, lb	Global buckling eigenvalue
2.60	5108	2.35
2.40	4971	2.13
2.20	4817	1.91
2.00	4653	1.70

the global buckling eigensolution and resulted in a final weight of 4653 lb. This final weight represents a 44-percent savings over the average weight (8367 lb) of all the feasible experimental matrix cases (those with a global buckling eigenvalue over 1.0).

7. Concluding Remarks and Recommendations

The following concluding remarks are based on the initial assumptions from other disciplines and the results of the design and analysis study.

The Taguchi design method and the finite element analysis method were successful in identifying which design parameters have the most influence on the weight and global buckling. The aerobrake weight and global buckling are sensitive to all the parameters, but particularly to the honeycomb thickness, the number of radial frames, and the material.

Utilization of the Taguchi method significantly reduced the number of experimental configurations. Without the utilization of the Taguchi design method and the L_{27} orthogonal matrix, 729 experiments would have been necessary to find the lightest weight combination instead of the 27 made in this study. The interactions and trends of the parameters could not have been captured without the use of the Taguchi method within the time constraints of the study.

Combining the Taguchi design method and the finite element analysis method provides an effective approach for conceptual-preliminary level aerobrake optimization studies. The average aerobrake weight of all the feasible experiments is 8367 lb, and the maximum feasible weight is 10 144 lb. The optimized structural weight of the aerobrake is 4653 lb, which is a weight savings of 3714 lb over the average aerobrake weight.

Global buckling is a critical failure criterion for lunar aerobrakes. The preliminary study showed that although the aerobrake structure could be sized to withstand the local failure criteria, the global buckling criterion could not always be satisfied.

The optimum level of the design parameters for minimizing weight is 10 frames, 7 rings, a 2.40-in. honeycomb core thickness, carbon-carbon material, spheroidal shape, and a diameter-depth ratio of 6.

Interactions occur between the honeycomb thickness, the shape, and the material. Changes in any of these parameters affect the impact of the remaining parameters.

Future structural design studies of lunar aerobrakes should include further considerations. Cost studies should be included since optimum weight configurations may not be synonymous with optimum cost. A thermal analysis of the aerobrake structure and its thermal protection system should be included to lend more detail to the weight estimations. Assembly and operational issues should be considered because they can have a dramatic impact on the weight and life-cycle cost of the configuration.

NASA Langley Research Center
Hampton, VA 23681-0001
September 29, 1992

References

1. *Synthesis Group on America's Space Exploration Initiative: America at the Threshold.* Superintendent of Documents, U.S. Government Printing Off., c.1991.
2. Braun, Robert D.; Powell, Richard W.; and Hartung, Lin C.: *Effect of Interplanetary Trajectory Options on a Manned Mars Aerobrake Configuration.* NASA TP-3019, 1990.
3. McDonnell Douglas Space Systems Co.: *Lunar Aerobraked Vehicle Operations & Cost Assessment, Phase 3 Report — Final Cost Assessment.* July 1991.
4. McDonnell Douglas Space Systems Co.: *Lunar Aerobraked Vehicle Operations & Cost Assessment, Phase 2 Report — LTV Design & Technology, Updated Cost Assessment.* Apr. 1991.
5. Tippett, L. H. C.: *Technological Applications of Statistics.* John Wiley & Sons, Inc., c.1950.
6. Taguchi, G.; and Konishi, S.: *Taguchi Methods® — Orthogonal Arrays and Linear Graphs.* American Supplier Inst., Inc., c.1987.
7. Sullivan, Lawrence P.: The Power of Taguchi Methods. *Qual. Prog.*, vol. XX, no. 6, June 1987, pp. 76–79.
8. Willie, R. H.: Landing Gear Weight Optimization Using Taguchi Analysis. SAWE Paper No. 1966, May 1990.
9. Peery, David J.; and Azar, Jamal J.: *Aircraft Structures, 2nd ed.* McGraw Hill, c.1982.
10. *Adv. Mater. & Process.* Vol. 137, issue 6, June 1990.
11. Phadke, Madhav S.: *Quality Engineering Using Robust Design.* Prentice Hall, 1989.

12. Taguchi, Genichi; Elsayed, Elsayed A.; and Hsiang, Thomas C.: *Quality Engineering in Production Systems*. McGraw-Hill Book Co., 1989.

13. *Taguchi Methods®—Introduction to Quality Engineering. Implementation Manual, Version 2.1*. American Supplier Inst., Inc., 1989.

14. McMillin, M. L.; Rehder, J. J.; Wilhite, A. W.; Schwing, J. L.; Spangler, J.; and Mills, J. C.: A Solid Modeler for Aerospace Vehicle Preliminary Design. AIAA-87-2901, Sept. 1987.

15. *Patran Plus User Manual—Release 2.5*. Publ. No. 2191025, PDA Engineering, Oct. 1990.

16. Bonner, E.; Clever, W.; and Dunn, K.: *Aerodynamic Preliminary Analysis System II. Part I—Theory*. NASA CR-182076, 1991.

17. Sova, G.; and Divan, P.: *Aerodynamic Preliminary Analysis System II. Part II User's Manual*. NASA CR-182077, 1991.

18. Brauer, G. L.; Cornick, D. E.; and Stevenson, R.: *Capabilities and Applications of the Program To Optimize Simulated Trajectories (POST)—Program Summary Document*. NASA CR-2770, 1977.

19. Whetstone, W. D.: *EISI-EAL Engineering Analysis Language Reference Manual—EISI-EAL System Level 2091*. Engineering Information Systems, Inc., July 1983.
Volume 1: General Rules and Utility Processors.
Volume 2: Structural Analysis—Primary Processors.

20. Cerro, Jeffrey A.; and Shore, C. P.: *EZDESIT—A Computer Program for Structural Element Sizing and Vehicle Weight Prediction*. NASP CR-1092, 1990.

REPORT DOCUMENTATION PAGE

Form Approved
OMB No. 0704-0188

1. AGENCY USE ONLY *(Leave blank)*	2. REPORT DATE	3. REPORT TYPE AND DATES COVERED
	December 1992	Technical Paper

4. TITLE AND SUBTITLE
Weight Optimization of an Aerobrake Structural Concept for a Lunar Transfer Vehicle

5. FUNDING NUMBERS
WU 593-11-11-01

6. AUTHOR(S)
Lance B. Bush, Resit Unal, Lawrence F. Rowell, and John J. Rehder

7. PERFORMING ORGANIZATION NAME(S) AND ADDRESS(ES)
NASA Langley Research Center
Hampton, VA 23681-0001

8. PERFORMING ORGANIZATION REPORT NUMBER
L-17120

9. SPONSORING/MONITORING AGENCY NAME(S) AND ADDRESS(ES)
National Aeronautics and Space Administration
Washington, DC 20546-0001

10. SPONSORING/MONITORING AGENCY REPORT NUMBER
NASA TP-3262

11. SUPPLEMENTARY NOTES
Bush, Rowell, and Rehder: Langley Research Center, Hampton, VA; Unal: Old Dominion University, Norfolk, VA.

12a. DISTRIBUTION/AVAILABILITY STATEMENT
Unclassified Unlimited

Subject Category 15

12b. DISTRIBUTION CODE

13. ABSTRACT *(Maximum 200 words)*
An aerobrake structural concept for a lunar transfer vehicle was weight optimized through the use of the Taguchi design method, finite element analyses, and element sizing routines. Six design parameters were chosen to represent the aerobrake structural configuration. The design parameters included honeycomb core thickness, diameter-depth ratio, shape, material, number of concentric ring frames, and number of radial frames. Each parameter was assigned three levels. The aerobrake structural configuration with the minimum weight was 44 percent less than the average weight of all the remaining satisfactory experimental configurations. In addition, the results of this study have served to bolster the advocacy of the Taguchi method for aerospace vehicle design. Both reduced analysis time and an optimized design demonstrated the applicability of the Taguchi method to aerospace vehicle design.

14. SUBJECT TERMS	15. NUMBER OF PAGES
Structural analysis; Taguchi method; Aerobrake	19
	16. PRICE CODE A03

17. SECURITY CLASSIFICATION OF REPORT	18. SECURITY CLASSIFICATION OF THIS PAGE	19. SECURITY CLASSIFICATION OF ABSTRACT	20. LIMITATION OF ABSTRACT
Unclassified	Unclassified		

NSN 7540-01-280-5500

Standard Form 298(Rev. 2-89)
Prescribed by ANSI Std. Z39-18
298-102

NASA-Langley, 1992